Fusion Energy Research with Lasers, Direct Drive Targets, and Dry Wall Chambers *

J.D. SETHIAN, S.P. OBENSCHAIN, M. MYERS, A J. SCHMITT, D. COLOMBANT, J. GARDNER, F. HEGLER, M. WOLFORD, J. GIULIANI, P. KEPPLE, and S. SWANEKAMP
Plasma Physics Division, Naval Research Laboratory, Washington, DC
D. WEIDENHEIMER, Titan Pulse Sciences Division, San Leandro, CA
D. WELCH and D. ROSE, Mission Research Corporation, Albuquerque, NM
S. PAYNE, C. BIBEAU, A. BARAYMIAN, R. BEACH, K. SCHAFFERS, B. FREITAS, W. SKULINA, W. MEIER, J. LATKOWSKI, J. LINDL, and L.J. PERKINS, Lawrence Livermore National Lab
D. GOODIN and R. PETZOLDT, General Atomics, San Diego, CA
F. NAJMABADI, M. TILLACK and R. RAFFRAY, University of California, San Diego
D. HAYNES, R. PETERSON, G. KULCINSKI, University of Wisconsin
A. NOBILE and J. HOFFER, Los Alamos National Laboratory
D. SCHROEN, Schafer Corp, Livermore, CA
C. OLSON, T. TANAKA, and T. RENK, Sandia National Laboratory
L. SNEAD, Oak Ridge National Laboratory

e-mail contact of main author: sethian@this.nrl.navy.mil

ABSTRACT. We are carrying out a coordinated, focused effort to develop Laser Inertial Fusion Energy. The key components are developed in concert with one another and the science and engineering issues are addressed concurrently. Significant progress has been made in this program: We are evaluating target designs that show it could be possible to achieve the high gains (>100) needed for a practical fusion system. These have a low density CH foam that is wicked with solid DT, and over coated with a thin high-Z layer. Significant advances have been made with the two types of laser are being developed: Krypton Fluoride (KrF) gas lasers and Diode Pumped Solid State Lasers (DPPSL). Both have the potential to meet the fusion energy requirements for rep-rate, efficiency, durability and cost. This paper also presents the advances in development of chamber operating windows (target survival plus no wall erosion), final optics (aluminum at grazing incidence has high reflectivity and exceeds required laser damage threshold), target fabrication (advanced foams and high Z overcoats), and target injection (new facility for target injection and tracking studies).

1. Introduction

We are carrying out a coordinated, focused effort to develop Laser Inertial Fusion Energy (Laser IFE). The approach is based on lasers, direct drive targets, and dry wall chambers. We are developing the key components for this concept in concert with one another and are addressing the science and engineering issues at the same time. This integrated approach ensures Laser Fusion Energy will be developed as a coherent system.

The attractiveness of this approach lies in its inherent simplicity, its separable architecture, and the modular nature of the laser driver. The targets are spherical shells, which in principal can be fabricated in a single droplet generator. Thus, they naturally lend themselves to automated, low cost production. Moreover, none of the target components need to be recycled. The first wall is a passive structure that does not have to hold vacuum. Not having to worry about vacuum

integrity allows the wall to be made in individual sectors that can be replaced during the plant lifetime. It also allows more choices for the first wall material, such as advanced composites that may have radiological advantages. The separable nature of the power plant allows the principal components to be developed separately before being integrated into the system. Just as importantly, it allows economical upgrades as new technologies are developed. The laser is modular, and would consist of a number (about 60) of identical beam lines. Hence it is only necessary to develop one of these lines to develop the entire system. All of these factors significantly reduce the development costs for this approach.

2. Progress

2.1 Target Physics

A typical high gain target design is shown in Figure 1 [1].

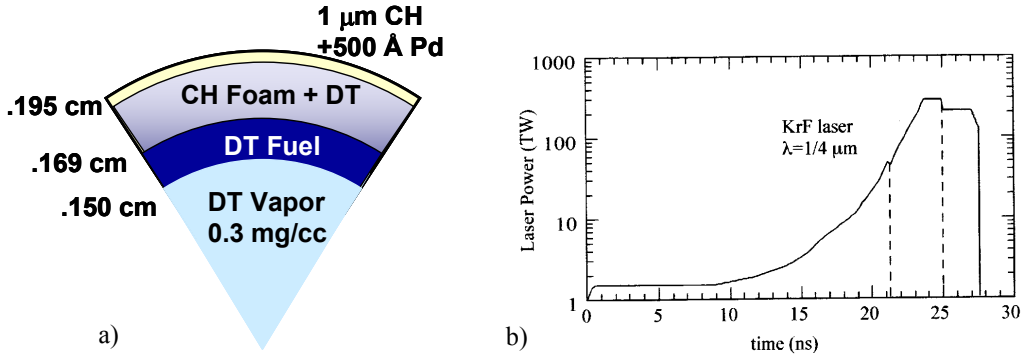

FIG.1. a) Typical NRL high gain target design and (b) laser pulse shape. Dashed lines are zoom points.

The current designs share several common features:

1. The laser pulse has a low intensity "foot" followed by a rise to maximum intensity.
2. The ablator is composed of a low density foam with DT wicked into it. The foam can significantly increase the laser absorption.
3. The design preheats the ablator by some means (shock, x-rays, or a combination). This raises the isentrope of the ablator, and hence lowers the growth rate of the Rayleigh Taylor instability. In some designs the ablator is preferentially heated, while the fuel remains on a lower isentrope. This increases the stability without materially reducing gain.
4. The laser is "zoomed:" the spot size is decreased in radius to match the compressing target.
5. The designs include a thin high Z layer (such as Pd) outside the target. This has been shown experimentally to significantly reduce the imprint of laser non-uniformities, and hence mitigates the seeding of hydrodynamic instabilities [2]. This is shown in Figure 2.

The high-Z material was originally chosen to be gold, but was later changed to palladium because the latter's permeability to hydrogen (DT) is important for target fabrication. Based on a number of calculations, any mixture of Au and Pd would present similar target performance; the only difference being the required thickness of the coating. The predicted 1-D gain of these targets, as a function of the Pd layer thickness, is shown in Figure 3. The figure also shows results from a second generation higher energy (400 MJ) target design

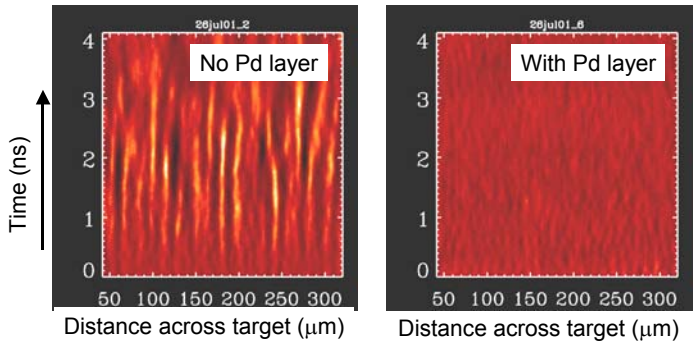

FIG.2. X-ray streak radiographs of ablatively accelerated planar targets show no measurable instability growth with 1200 Å Pd layer on target front surface.

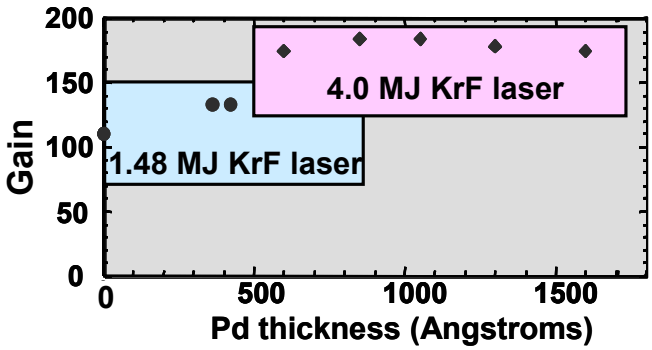

FIG. 3.Target gain as a function of Pd thickness.

We are using the NRL FAST series of codes to evaluate these targets with high-resolution 2D fully integrated simulations. These resolve all the wavelengths relevant to the hydrodynamic instability. We account for all known sources of non-uniformity: inner and outer surface roughness (based on NIF pellet specifications), laser imprint from optical smoothing (based on ISI and SSD modeling) and low-mode laser pointing and power imbalances (based on modeling from the NIF laser system). Simulations are ongoing for the NIF base-line pellet design, and are beginning for the NRL high-gain KrF-driven pellets. Figure 4 is an example calculation.

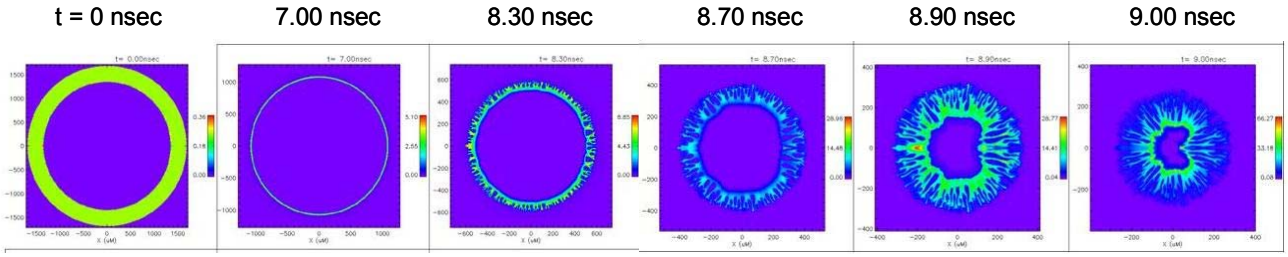

FIG.4. 2-D simulations of a NIF pellet implosion. Gain = 18.

We have also carried out 2-D single mode calculations for a 400 MJ target design with LASNEX. This target is slightly larger than that shown in Figure 1, and has a 6 μm thick pure CH outer layer. The calculations show that the stability is enhanced by adding a single high intensity spike early in the foot of the laser pulse. This prepulse shock heats the ablator to a higher isentrope (with a concurrent reduction in Rayleigh Taylor growth) but decays before reaching the fuel.

2.2. KrF Laser

KrF laser development is being carried out with the Electra Program at NRL. The key components are: an efficient and durable pulsed power system, a durable electron beam emitter (cathode), a long life, high transmission foil support structure (hibachi), a recirculator to cool and quiet the laser gas, and long life optical windows. Electra should produce 400-700 J in 100 nsec. The technologies will be directly scalable to a fusion power plant sized laser beam line.

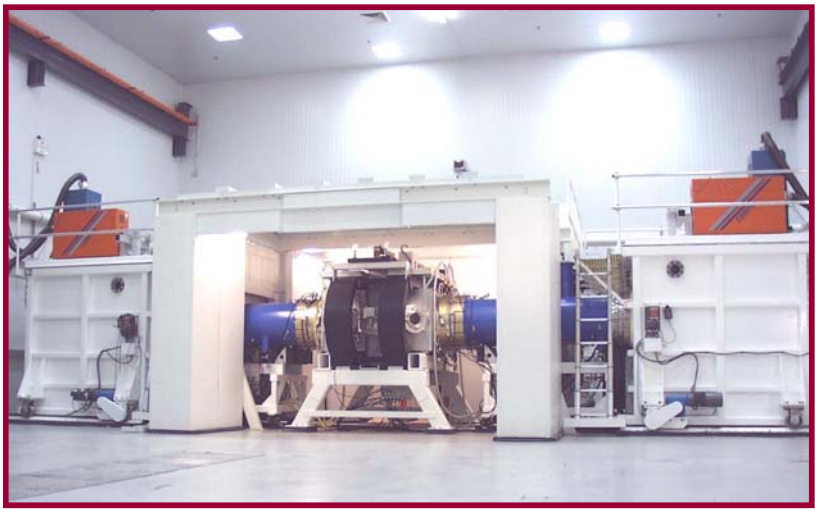

FIG. 6. The Electra Laser Facility.

We have built a first generation pulsed power system to develop the laser components. The system produces two 500 keV, 100 kA, 100 nsec electron beams, each 30 cm high by 100 cm wide. The pulsed power system can run at 5 Hz for 5 hours (100,000 shots) and e-beam runs of several thousand shots are commonplace. The facility is shown in Figure 6. Although considerable progress has been made in all areas, we have made three significant advances in the pulsed power, hibachi, and KrF physics modeling.

2.2.1. Advanced Pulsed Power

We have developed an all new solid state, laser triggered switch that will become the basis for a pulsed power system that can meet the IFE requirements for rep-rate, durability, and cost. The switch uses a four-junction silicon device that is optically triggered by two diode lasers. The lasers flood the entire switch volume with photons, whose energy is just above the band edge of the silicon. This gives ultra fast switching times (compared to other solid state switches), on the order of 100 nsec. The lasers are kept on during the entire electrical pulse, which results in high efficiency. Using a four junction device enables operation at voltages of 20 kV. We call this device a *Laser Gated and Pumped Thyristor.* For the first tests, we modified an off-the-shelf Thyristor to accommodate a single diode laser and the necessary optical coupling. The switch operated at 3.2 kV for 10^5 shots at 5 Hz. The current density was 2.7 kA/cm^2 (121% of the IFE requirement) and rate of rise of was 1.4 x 10^{10} A/sec/cm^2 (154% of the IFE requirement). We then built a second generation switch using advanced, purpose-built construction techniques, with two-sided pumping. This switch has operated at 15.2 kV and held 24 kV in a pulse charge. This revolutionary pulsed power switch has a wide range of other pulsed power applications.

2.2.2. Hibachi (foil support structure)

We have developed a hibachi concept that demonstrates energy deposition transmission efficiency of up to 75% on Electra (500 keV), with the potential to go to greater than 80% at full system operating voltages (750 keV). The energy deposition efficiency is defined as the ratio of the energy deposited in the laser gas divided by the energy in the diode. The high transmission efficiency was achieved with two innovations: 1) Eliminating the anode foil on the diode side of the hibachi structure, and 2) Patterning the electron emitter into strips so the beam "misses" the hibachi ribs. While these are conceptually simple, they are difficult in practice: The beam strips spread due to the highly non-uniform electric fields caused by eliminating the anode, and the beam rotates and shears due to the applied magnetic field. We compensate for these by narrowing the emitter and "counter-rotating" the emitters so the beam "strips" are propagating parallel to the ribs when they get to the hibachi. This concept is shown in Figure 7. As a side note, patterning the beam into strips also delays and reduces the "transit time" instability that is characteristic of large area electron beams.

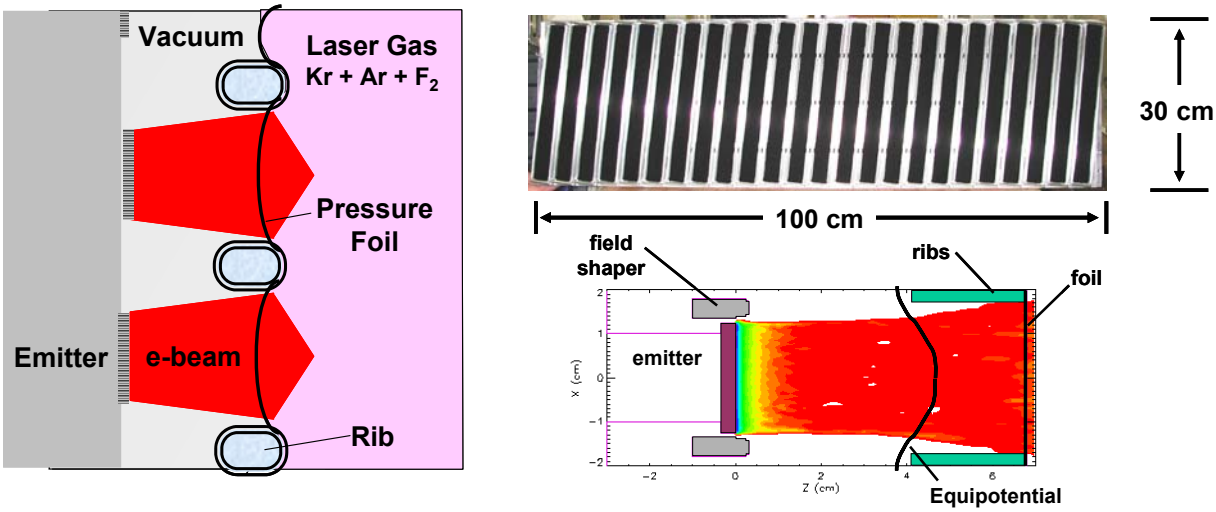

FIG. 7. Drawing of hibachi concept (left,) photo of cathode showing the counter-rotated emitter strips (upper right), and LSP modeling of beam propagation past ribs (lower right)

While the topology of the cathode strips can be determined empirically, this does not give us the predictive capability needed to design larger systems. This is a complex phenomenon to model and requires a full 3-D PIC simulation of the rib structure, laser gas, and magnetic field. We achieved this by running the Large Scale Plasma (LSP) code developed by MRC, Albuquerque on our own massively parallel homegrown processors. The simulations accurately predict both the cathode counter rotation angle and the energy deposition efficiency. A simulation of a beam "strip" is also shown in Figure 7.

2.2.3. KrF Physics Code development

We have developed the "Orestes" KrF Physics code to both predict the behavior of Electra and to design full scale (30-100 kJ) systems. Orestes has been benchmarked against a wide range of KrF experiments under different conditions. Using the experimental energy depositions, Orestes predicts the Electra to produce 550 J to 850 J, depending on the experimental parameters.

2.3. Diode Pumped Solid State Laser

Diode Pumped Solid State Laser development is being carried out with the Mercury Program at LLNL. The ultimate goal is to produce a 100 J, 10 nsec, 10 Hz, 10% efficient laser. Like the Electra KrF laser, the technologies developed on Mercury are scalable to a full size power plant laser. To achieve the goals of Mercury, three key technologies have been developed: high peak-power diode arrays, $Yb^{3+}:Sr_5(PO_4)_3F$ (Yb:S-FAP) crystalline gain slabs, and helium gas cooling of the gain media. The facility is shown in Figure 9.

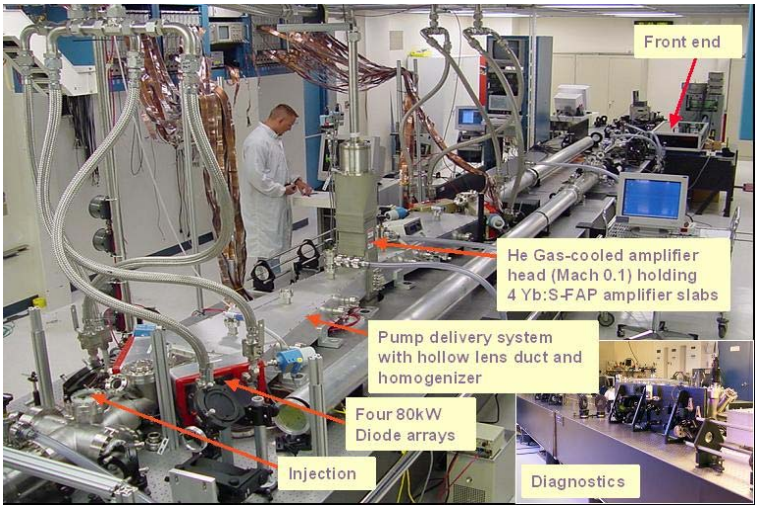

FIG. 9. The Mercury Laser with a single amplifier head (partially fitted with Yb:S-FAP slabs). In this configuration, the system produces 20 J of energy per pulse.

The system is schematically illustrated in Figure 10. The diode array light is guided to the amplifier through multiple reflections within a hollow lens duct and homogenizer. The diode pump light is delivered to the Yb:S-FAP amplifier slabs potted into aerodynamic vanes, which are cooled by helium gas flowing at Mach 0.1. By means of angular multiplexing, the beam is injected into the main cavity and relay-imaged two times through the amplifier head. The beam is then re-injected via a U-turn loop (called a "reverser"), which contains a birefringence-compensated Pockels cell (used for ghost and parasitic beam suppression). This allows the beam to pass through the amplifier two more times. In collaboration with the University of

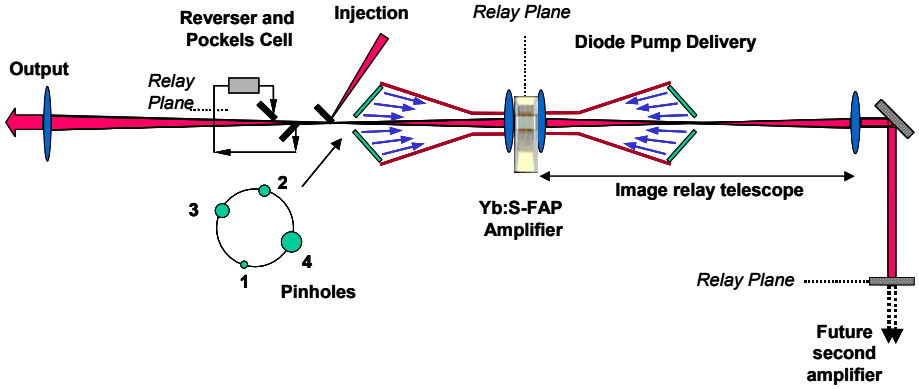

FIG. 10. Schematic of the Mercury Laser.

Rochester, we have developed a device for "spectral-sculpting" the input beam, so as to maximize the output bandwidth for beam smoothing. We have developed a dark field diagnostic, which operates at 10 Hz to monitor the system for the onset of damage. To date, we have activated one of two amplifier heads and generated 20 J in a 20 nsec pulse.

Significant improvements have been made in the growth of the ytterbium-doped strontium fluorapatite (Yb:S-FAP) crystals. While these Czochralski-grown crystals were initially plagued by a number of growth-related defects, they have been brought under control with newly developed procedures for the fabrication of the S-FAP crystal slabs, including water cutting, acidic-polishing and diffusion-bonding.

Significant advances have been made with the Mercury Laser system. Four diode arrays have been activated with each delivering 80 kW of peak power in a 750 μs pulse. The first set of diode arrays and pump delivery optics have been completed, tested, and found to meet or exceed all specifications. An overall transfer efficiency of 83% through the pump delivery system was achieved, and the pump homogeneity matches our ray-trace models. A birefringence-compensated average power KD*P Pockels cell was fabricated and meets the 200:1 extinction requirement at 100 W average power. Four of the seven 4x6 cm Yb:S-FAP slabs are currently installed in the amplifier. An example of performance results for one amplifier head appears in Figure 11. Full power operation of this amplifier head is anticipated by early 2003, and is anticipated to produce 30 J at 10 Hz. To achieve this goal, wave front correction plates will be installed to remove the amplifier distortions; initial demonstrations of static wave front correct have been quite encouraging. The second amplifier head is expected to be activated in 2003.

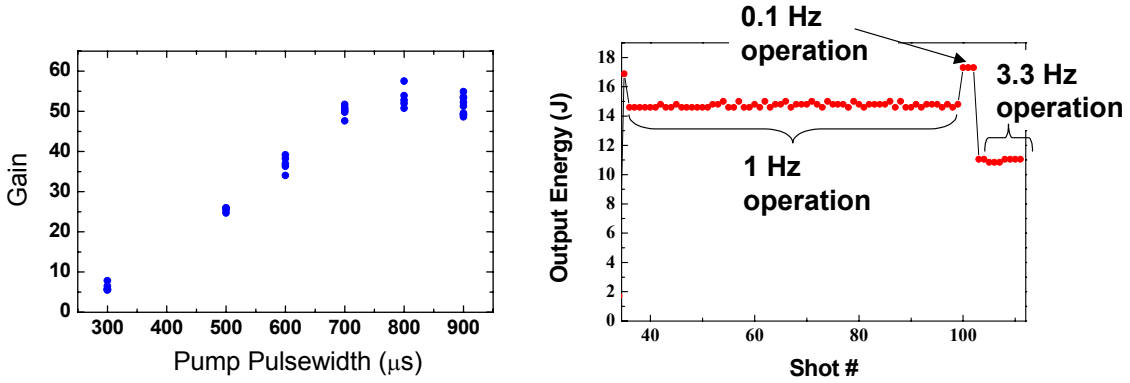

FIG.11. Small signal gain through the system (left). Operations plot showing output energy and stability for various repetition rates (right).

The Mercury Laser crew gratefully acknowledges the support of Coherent Inc. for laser diode bars, PolyScientific Northrop-Grumman for crystal growth, Onyx Corp. for diffusion-bonding the crystals, and Directed Energy Inc. for the diode pulsars.

2.4. Chamber Development

We have established an operating window for target yield, chamber radius, and chamber gas pressure that will avoid first wall vaporization, allow target injection without compromising the frozen DT fuel, and operate at a reasonable efficiency. Figure 12 gives the results for a tungsten armored first wall and a 154 MJ target. The tungsten stays well below the melting temperature of 3410°C. Note there is no gas inside the chamber.

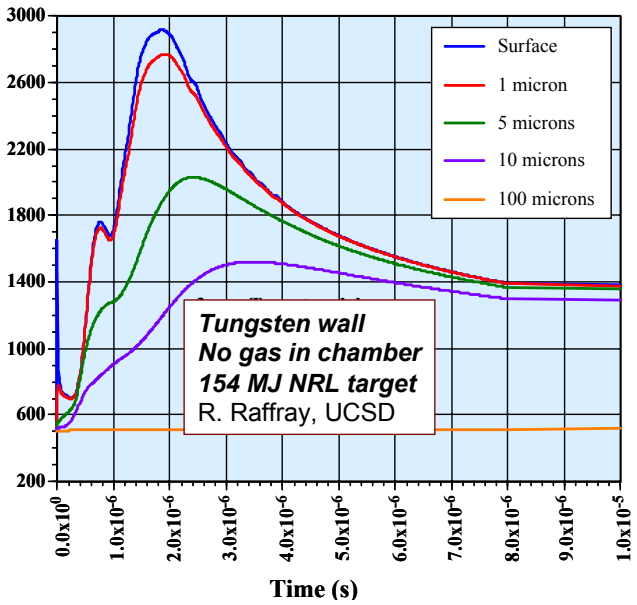

FIG. 12: Predicted temperature profiles of first wall in an IFE chamber

Similar results were obtained for a C armor except that the initial photon-induced peak is much smaller since the photon energy deposition goes deeper inside the C and the maximum temperature is <2000°C with an associated annual sublimation loss of less than 1 μm.

While the identification of an operating window is a major step, there are still significant challenges to be met in establishing a viable chamber concept:

a. The results are highly dependent on simulations of complex physical processes (in particular the materials response to the target emission) which in turn are based on codes that have not been well benchmarked under relevant conditions.
b. Long term material behavior, is an issue, in particular tritium retention for carbon and helium retention for tungsten.
c. We do not yet have a self consistent operating window for the higher energy (400 MJ) target designs. In that case 80 mTorr of xenon is required in the chamber, while *current* estimates are the gas needs to be less than 10 mTorr in order not to compromise target injection.

2.4.1 Code Validation of Materials Response

In order to benchmark our code predictions of material damage thresholds, we have exposed candidate chamber first wall materials to ions and x-rays at fusion relevant fluences and spectra.

This past year we performed exposures with the Z (single shot x-rays) and RHEPP (repetitively pulsed ions) facilities at Sandia. Table II compares the experimental results, theoretical predictions, and anticipated threat from the two types of high gain targets shown in Figure 3.

TABLE II: SUMMARY OF EXPOSURES OF CANDIDATE FIRST WALL MATERIALS

	Material	Predicted Ablation Threshold	Measured Ablation Threshold	Measured Roughening Threshold	Predicted Threat to wall[1]	
					154 MJ target	400 MJ target
X-rays (10 nsec exposure)	Pyrolitic Graphite	4.0 J/cm^2	3.5 - 4 J/cm^2	2.5 J/cm^2	0.40 J/cm^2	1.20 J/cm^2
	Tungsten	not done yet	2 J/cm^2	1.3 J/cm^2		
IONS (60 nsec exposure)	Pyrolitic Graphite	4.5 J/cm^2	3.5 - 4 J/cm^2	2.5 J/cm^2	1.41 J/cm^2	3.52 J/cm^2
	Tungsten (pure)	4.75 J/cm^2	5 J/cm^2	1.25 J/cm^2		
	Tungsten (+ 25% Re)	4.75 J/cm^2	5 J/cm^2	3.5 J/cm^2		

1. Assumes wall is at 6.5 m radius. Corrected for pulse width: X rays: Z and IFE target, both 10 nsec, hence no correction. Ions: RHEPP 60 nsec, IFE target: 2.1 μsec. We reduced the IFE threat by the square root of time difference, about six fold.

The measured ablation thresholds are close to the code predictions. The x-ray roughening threshold for both materials is above the predicted IFE threats for both targets, and the ion roughening threshold is above the predicted threat from the 154 MJ target. W+Re is the most robust, and has a roughening threshold that is even above the ion threat from the high yield target. (Although we note that Re has radiological issues).

We are also concerned about the so-called sub-threshold x-ray damage that becomes important only after many cycles. This will be studied with the new repetitive x-ray source XAPPER, which is being installed at LLNL. The source delivers high fluences of low-energy (100-500 eV) x-rays to a sample and operates at up to 10^6 pulses at 10 Hz.

2.4.2 Long Term Material Behavior

A major concern with carbon as armor is the tritium inventory due to tritium co-deposition in colder regions. On this basis a refractory metal such as W is preferable. However, the issue of He implantation must be addressed. The large fluxes of He ions can result in a 1 to 1 ratio of W:He within about 100 days of operation assuming a 1 μm implantation depth. This would lead to failure of chunks of armor. We are evaluating several solutions, including operation at high enough temperature for He to be mobile in W or by using very fine porous structure to provide a very short migration path for He to be transported to open porosity and back to the chamber.

2.4.3 Magnetic Deflection

An option for the protection of the chamber wall and/or final optics that is the use of magnetic fields. For moderate (~1 T) uniform magnetic fields, one can limit the 1-D plasma expansion to ~4 m, greatly reducing the ion fluxes on the wall. 3-D effects and production of neutrals, however, are expected to reduce the effectiveness of the approach. Protection of the final optics may be accomplished with a two-prong approach: gas puffs on the order of several Torr-m are sufficient to stop the heavier, charged particles, while small magnets with fields of <0.5 T are capable of deflecting the lighter particles, such as the He ions.

2.4.4 Chamber Dynamics

In a rep-rated laser-fusion facility, the pulse repetition rate is limited by the time it takes for chamber environment to return to a sufficiently quiescent and clean state following a target explosion that a second shot can be initiated. Many physical phenomena with different time scales occur in the chamber following the target implosion. In the first few microseconds, the x-ray burst and ions from the fireball traverse the chamber, depositing their energy in the chamber constituents and finally on the chamber wall. After this phase, the chamber environment evolves mainly in the hydrodynamics time scale and a new equilibrium condition is achieved after certain time interval (typically 100-200 ms). The aim of chamber dynamics and simulations research is to understand the chamber evolution and dynamic over this "longer" time scale and understand the constraints imposed by the chamber dynamics. We have developed a 2-D chamber dynamics and clearing code for this purpose. Some examples of the computational capabilities of the code are shown in Figure 13.

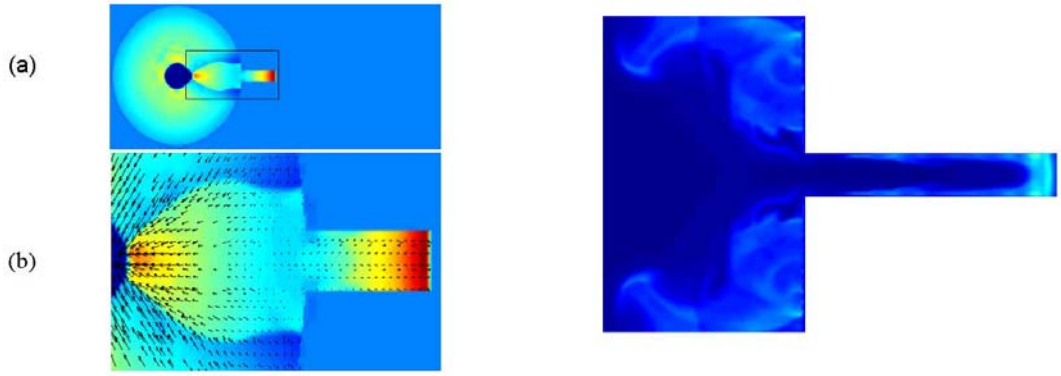

FIG. 13. Conditions 1.6 ms after the target blast. Left: Chamber a) pressure and b) velocity distribution. Right: Density distribution around the entrance of the laser beam channel.

2.5. Final Optics

Our front runner final optic concept is a grazing incidence pure aluminum surface bonded to a cooled, neutron transparent substrate. Operation at a shallow angle (~85˚) gives the dual advantage of reduced absorption for s-polarized light and lower average fluence on the surface due to the large footprint of the beam. As seen in Figure 14, experiments have established that, at least in small laser spot sizes, we can significantly exceed the required laser damage threshold (> 50 J/cm^2 vs. the required 5-8 J/cm^2).

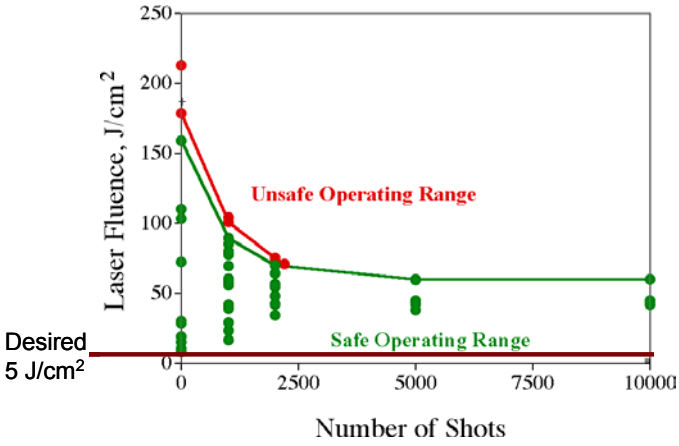

FIG. 15. Laser-induced damage threshold (fluence is measured normal to the beam).

In addition to laser damage, the final optic is subjected to neutrons, x-rays, gamma rays and charged particles. The threats on the optic at 20 m from chamber center are significantly reduced compared to that on the chamber walls at 6.5 m. However they are important in view of the stringent beam quality requirements for target implosion. We will assess the effects of these threats. If they are found to be serious, we will then pursue mitigation techniques such as fast shutters, magnetic deflection, etc.

We are also investigating transmissive optics. Here the key issue is absorption center production by either neutrons or gammas. Our work has concentrated on SiO_2, CaF_2 and Al_2O_3. For each of these, color center accumulation rapidly leads to significant laser absorption at both the KrF and DPSSL frequencies. We found, however, that heating an SiO_2 optic allows the defect concentration to saturate at acceptable levels, at least at the DPSSL wavelength of 351 nm. For example, a large area, 0.5-mm-thick Fresnel lens operated at a temperature of 500°C, is expected to have a laser absorption of <1%. The absorption is too high for KrF at 248 nm.

2.6. Target Fabrication

We have concentrated on developing target fabrication techniques that can eventually scale to mass production at low cost. For example, we have developed advanced divinyl-benzene foam shells using micro encapsulation, a process well suited to mass production. Up to 300 shells, with the proper diameter, density, and wall thickness, have been produced in a single batch. (The material was chosen because it meets the requirements for low oxygen content and straightforward over coating.) In the coming year we will work on concentricity, reproducibility, and over-coating. Measurements show an Au-Pd alloy meets the requirements for DT permeation times (almost as good as pure Pd), and has high IR reflectivity (almost as good as pure gold) to help the target survive as it traverses the hot chamber. A high gain target will require a smooth surface (less than 1 um RMS) on the inner surface of the DT ice layer. We are developing a batch process based on a fluidized bed technology. Experiments with a room temperature surrogate (oxalic acid) and an infra-red heat source (to mimic the natural heat from tritium decay) have demonstrated the feasibility of this. We predict the total tritium inventory in a laser fusion power plant could be under 300 g. This is below the normally acceptable value of 1

kg. We estimated the cost of producing a direct drive target of about 16.6 cents each. This is well under the 25 cents called for by power plant studies.

2.7 Target Injection

We have started construction of a system to study target injection and tracking (See Figure 15). The injector is designed to accelerate any IFE target (both indirect and direct drive) and thus is important for any repetitively pulsed IFE/ICF concepts. For direct drive targets, we have demonstrated the concept of a separable sabot to protect the target during acceleration. We are also measuring both the mechanical properties of solid DT (for prediction of target survival during the high g-loading of injection) and the thermal properties (to determine target survival).

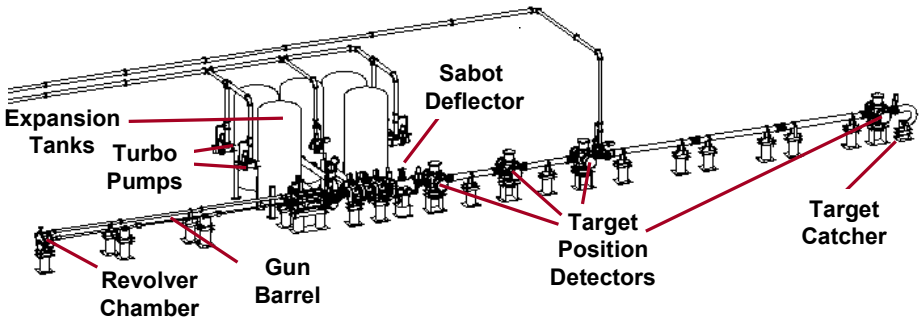

FIG.15. Drawing of target injection and tracking system (under construction).

3.0 Development of Laser Fusion Energy

The work discussed here is the first of a three phase program to develop laser fusion energy: Phase I is basic science and technology development. Phase II is full scale technology development and partial integration. Phase III is a fully integrated engineering test facility (ETF). Specific goals and milestones must be met before advancing from one phase to the next. Each phase represents increasing confidence, decreasing technical risk, and increasing cost. In all phases the various components will be developed in concert with one another to ensure we are developing laser fusion energy as an integrated system. The last phase (ETF) would demonstrate repetitive fusion power and is expected to start within the next 10-15 years.

4.0 Acknowledgements

This work is sponsored by the US Department of Energy, NNSA/DP.

5.0 References

[1] S.E. Bodner, D. G. Colombant, A.J. Schmitt, and M. Klapisch, "High Gain Direct Drive Target Design for Laser Fusion" Phys of Plasmas **7**, (2000) 2298.

[2] S.P.Obenschain, D. Colombant, M. Karasik, C. J. Pawley, V. Serlin, A. J. Schmitt, J. Weaver, J. H. Gardner, L. Phillips, Y. Aglitskiy and Y. Chan, J. P. Dahlburg, M. Klapisch, "Effects of Thin High-Z Layers on The Hydrodynamics of Laser-Accelerated Plastic Targets" accepted for publication in Physics of Plasmas.